ISSN:3007-9640 DOI: https://doi.org/10.70114/acmsr.2025.3.1.P177

Simulation Analysis of GNSS-R Sea Surface Coverage Performance Based On Low Orbit Satellites

Siqi Gu, Jin Qin, and Bo Zhou

Shanghai Aerospace Electronic Technology Institude, Shanghai, 201109, China;

gusiqihao@163.com

Abstract. GNSS-R (Global Navigation Satellite System-Reflection) remote sensing technology has been widely applied in fields such as earth science, meteorology, and oceanography in recent years. Its coverage performance directly affects global monitoring capabilities, data acquisition continuity, and multi-scenario applicability. This article simulates and analyzes the coverage performance of the ground geometry relationship of the GNSS-R payload carried by low orbit satellites. Through the joint-simulation method of STK and Matlab, the visibility of specular reflection signals and sea surface coverage performance under different orbital heights, antenna beam numbers, working hours, spatial resolutions, etc. are analyzed. The results show that the low orbit GNSS-R payload can efficiently detect global marine environmental elements. The 4-beam antenna based on single satellite can achieve over 80% global sea surface coverage and measurement accuracy better than 10cm. The data can evaluate the coverage efficiency and measurement accuracy of sea surface parameters for other different payloads design, and through multi-satellite networking can further improve coverage efficiency and measurement accuracy.

Keywords: GNSS-R; Low Orbit; Sea Surface Parameters; Coverage Efficiency; Joint-Simulation.

1. Introduction

GNSS-R (Global Navigation Satellite System-Reflection) technology utilizes the principle of dual-base radar detection, using the L-band signal of the Global Navigation Satellite System (GNSS) as the transmission source, simultaneously receiving and processing direct signals from GNSS satellites and reflected signals from the Earth's surface through a space-based platform. By analyzing the characteristic differences between the direct signals and reflected signals to obtain the surface parameters. As a new remote sensing technology, GNSS-R can detect multi-elements in areas that are difficult to cover such as oceans and polar regions with traditional observation methods [1,2].

In September 2003, the UK-DMC (United Kingdom-Disaster Monitoring Constellation) satellite launched by the UK fully validated the feasibility of receiving GPS reflection signals from low orbit satellites [3]. In July 2014, the UK validated the DDM (Doppler Delay Mapping) technology in satellite environments by launching TDS-1, which was equipped with a GNSS remote sensing receiver [4]. In December 2016, NASA (National Aeronautics and Space Administration) launched the CYGNSS (Cyclone Global Navigation Satellite System) hurricane monitoring satellite, and achieved hurricane detection within the 35° latitude range of the global ocean through eight-satellite networking [5].

The development of GNSS-R technology has promoted its commercial application prospects, and its application value is directly reflected in the spatial coverage performance of GNSS-R signals [6,7]. The advantages of high coverage are as follows:

(1) Realize continuous observation of the same area, provide long-term series data, and apply to the long-term environmental change research;
(2) Quickly respond to emergencies, and apply to disaster monitoring;
(3) Combining with other remote sensing technologies to provide more comprehensive data, improve detection accuracy and reliability.

This article simulates the coverage of the ground geometry relationship of the GNSS-R payload carried by low Earth orbit satellites, and provides analysis results on the visibility of specular reflection signals, sea surface coverage, and the impact on the accuracy of sea surface height

ISSN:3007-9640 DOI: https://doi.org/10.70114/acmsr.2025.3.1.P177
detection. The rest of the paper is organized as follows. Section 2 briefly describes the theory of satellite remote sensing coverage area. Section 3 introduces the process of joint-simulation method and satellite selection strategy. Numerical simulation data and analysis results are provided in Section 4. Finally, conclusions are drawn in Section 5.

2. The theory of Satellite Remote Sensing Coverage Area

GNSS-R receivers use antennas with different gains to receive remote sensing reflection signals. Different antennas have different half power beam-width (at -3dB power level points), and their coverage range (Footprints) are also different [8]. Meanwhile, the coverage range is also related to the height and field of view of the antenna, as shown in the diagram below. Different remote sensing platforms have different antenna configurations and field of view.

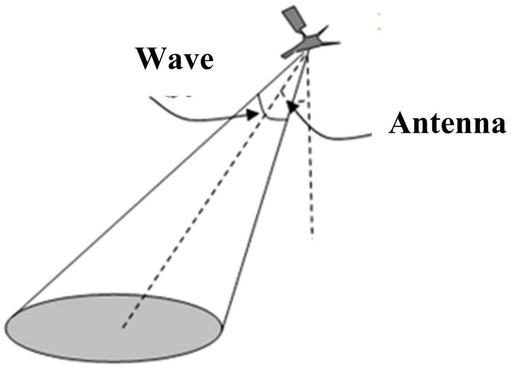

Fig. 1 Schematic diagram of coverage area

The antenna used in space-borne GNSS-R receivers is usually implemented through digital beamforming antennas, which have the ability to scan beams and the coverage area is determined by the scanning range of the antenna. The schematic diagram of satellite in orbit operation is shown below.

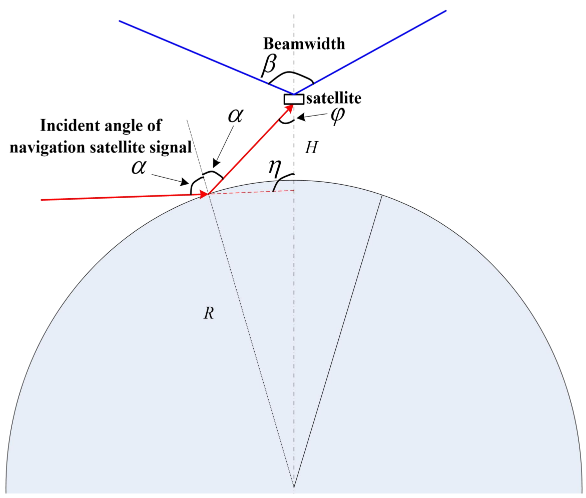

Fig. 2 Geometric relationship of the space-borne reflected signal receiving antenna

According to geometric relationships, the calculation formula is as follows. Where H is the satellite orbit altitude, R is the radius of the Earth, α is the angle of incidence of navigation satellite signals, β is the beam-width of the RHCP (Right-Hand Circular Polarization) antenna, φ is the scanning angle, and η is the angle between the incident signal and the satellite's Z-axis.

$$\alpha = \arcsin\left(\frac{H+R}{R}\sin(\varphi)\right)$$

$$\eta = 2\alpha - \varphi$$

ISSN:3007-9640 DOI: https://doi.org/10.70114/acmsr.2025.3.1.P177

According to the system detection principle [9,10], the GNSS-R receiver must simultaneously receive the direct signals and reflected signals of the same navigation satellite. Therefore, it is necessary to ensure that $\eta \leqslant \beta/2$, otherwise even if the LHCP (Left-Hand Circular Polarization) antenna can receive the specular reflection signals of the navigation satellite, the RHCP antenna cannot capture the satellite.

3. Simulation Process

Through the joint-simulation method of STK and Matlab, the remote sensing coverage of GNSS-R payload carried by low orbit satellites was analyzed. The flowchart of the simulation is shown in Fig. 3, where the simulation of GNSS satellite orbit and LEO orbit were implemented through STK, and the geometric relationship of the receiver and transmitter, as well as the calculation of specular reflection points, were implemented in Matlab.

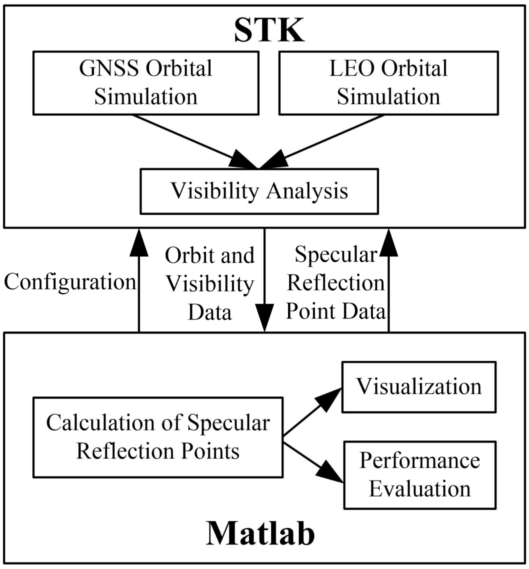

Fig. 3 The flowchart of simulation

The simulation processing flow is as follows:

(1) Using Matlab to configure the space-borne GNSS-R scenario parameters which is needed in STK;
(2) STK completes GNSS orbit simulation and LEO orbit simulation, uses parameters such as orbit, antenna, GNSS constellation, etc. for visibility analysis, and feeds back the orbit and visibility data to Matlab;
(3) Using Matlab to calculate the geometric relationship between GNSS constellations and LEO constellations, select GNSS satellites based on antenna beams and satellite selection strategies, and then calculate the position of the specular reflection points;
(4) Finally, generate visual results and complete the performance evaluation of GNSS-R remote sensing coverage and measurement accuracy.

The satellite selection strategy in simulation is based on the following points:

(1) At the simulation time, if the number of visible reflected signals is less than 4, discard all reflected signals at that time;
(2) At the simulation time, if the number of visible reflected signals is between 4 and the number of beams n, select all reflected signals at that time;
(3) At the simulation time, if the number of visible reflected signals exceeds the number of beams n, use the elevation angle for descending order, select the first n reflected signals.

ISSN:3007-9640 DOI: https://doi.org/10.70114/acmsr.2025.3.1.P177

4. Simulation and Result Analysis

Due to for different orbital heights, the visibility of reflected signals varies, which directly affecting coverage performance. Therefore, firstly simulates the impact of different orbital heights on visibility. The simulation considered the number of GNSS after the modernization of GPS and the completion of the Beidou Global System. GPS consists of 31 satellites, while Beidou has a total of 35 satellites (27 medium orbit+3 inclined orbit+5 geostationary orbit), utilizing the complete GPS constellation and 27 medium orbit satellites of the Beidou constellation.

The orbital setting parameters are as follows: the orbital eccentricity is 0, the orbital inclination is 98 °, the perigee angle is 0, and the ascending node right ascension is 264.252 °. The antenna gain is 20dB, and the scanning angle range is ± 45 °. As shown in Fig. 4, it can be seen that within the low orbit range, the statistical average of the visible number of reflected signals in the same area is proportional to the height.

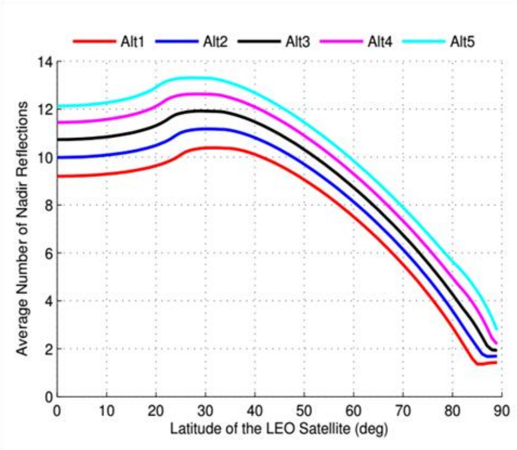

Fig. 4 The visible number of reflected signals in different satellite orbit altitude (Curve from bottom to top: Alt1: 500km, Alt2: 750km, Alt3: 1000km, Alt4: 1250km, Alt5: 1500km)

Based on the results in Fig. 4, set the simulated orbit altitude to 900km, and analyze the visibility of GNSS reflection signals under conditions such as single satellite and multi satellite networking, different working hours and different navigation satellite signal sources. The working hour is set to 1/5/10 days, and the number of satellites is set to 1/3. The visibility of reflected signals was analyzed for three scenarios: Beidou, GPS, and Beidou+GPS constellations.

The results are summarized in Table 1. The results show that the working hour has no effect on the visibility of reflected signals. As the number of navigation satellites increases, the visible reflected signals will superimpose, and the stability will be higher. For multi satellite networking, the number of reflected signals at the same time is proportional to the number of satellite networking. Therefore, through multi satellite networking, the visible number of reflected signals can be increased, thereby improving coverage efficiency and measurement accuracy.

Table 1 The statistical table of Reflected signal visibility

Number of constellations	Working hour/day	navigation satellite	Visible quantity of reflected signals	Mean value
1	1/5/10	Beidou	2~7	4~5
1	1/5/10	GPS	1~10	5~6
1	1/5/10	Beidou +GPS	4~16	10
3	1/5/10	Beidou	9~17	13
3	1/5/10	GPS	8~26	17
3	1/5/10	Beidou +GPS	20~42	31

Simulate the global sea coverage with single LEO satellite, the parameter settings are as follows. The orbit altitude is 900km, the working hours are 10/20/30/50/90 days, the number of antenna

ISSN:3007-9640 DOI: https://doi.org/10.70114/acmsr.2025.3.1.P177
beams is 4/8/12, using the Beidou+GPS+Galileo constellation, and the measurement spatial resolution is 10/20/40/110km^2. The measurement spatial resolution mentioned in this article refers to when processing GNSS-R remote sensing data, each retrieved sea surface height value corresponds to a position coordinate, dividing the Earth's surface area into fixed sized grids, that is the measurement spatial resolution. According to the boundary of the grid, the retrieved sea surface height value is assigned to a fixed grid cell. The sea surface height value represented by this grid cell can be obtained by averaging, differencing, fitting, and other methods from multiple retrieve values within the same grid cell.

The visualization results of the simulation are shown in Fig. 5, with red area indicating the coverage area. The final single satellite coverage and altimetry accuracy statistics are respectively shown in Table 2 and Table 3. The results indicate that the low orbit GNSS-R payload can efficiently detect global marine environmental elements. Considering factors such as weight and power consumption in practical in-orbit applications, the results show that a 4-beam antenna can achieve global sea coverage greater than 80% and measurement accuracy better than 10cm under single satellite. Meanwhile, the data can be used to evaluate the coverage efficiency and surface parameter measurement accuracy for different payload designs.

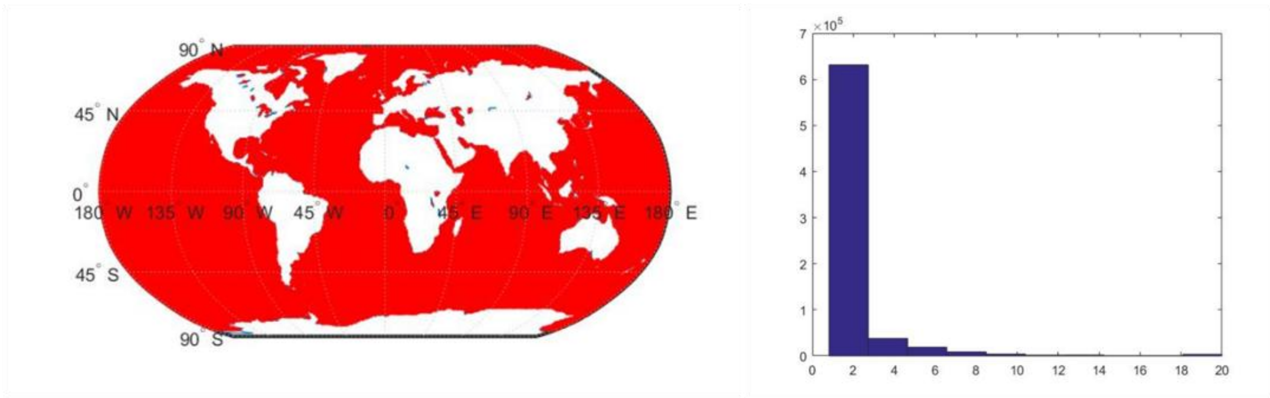

Fig. 5 Sea surface coverage rate of 98.76% (Left, red indicates coverage area); Statistics of altimetry accuracy distribution (Right)

Table 2 The statistical table of sea coverage rate results

Number of beams	Measurement spatial resolution/km^2	Coverage rate				
		10days	20days	30days	50days	90days
4	10	21.69%	36.59%	46.64%	60.95%	75.91%
	20	38.88%	57.88%	68.23%	78.65%	85.61%
	40	51.07%	69.58%	77.85%	84.00%	87.18%
	110	82.55%	86.7%	87.52%	87.99%	88.25%
8	10	37.56%	57.00%	68.33%	80.69%	88.45%
	20	60.33%	78.39%	85.25%	89.75%	91.52%
	40	72.76%	85.98%	89.53%	91.27%	92.12%
	110	90.50%	91.88%	92.51%	92.92%	93.54%
12	10	50.54%	71.83%	82.15%	91.30%	95.60%
	20	75.76%	90.86%	95.4%	97.04%	97.77%
	40	87.21%	95.85%	97.29%	97.86%	98.17%
	110	97.89%	98.32%	98.36%	98.54%	98.76%

Table 3 The statistical table of altimetry accuracy results

Number of beams	Measurement spatial resolution/km^2	Altimetry accuracy/cm				
		10days	20days	30days	50days	90days
4	10	75.31	53.52	43.48	33.68	25.10
	20	37.66	26.63	21.74	16.84	12.55
	40	20.92	17.25	12.08	9.36	6.97

ISSN:3007-9640 DOI: https://doi.org/10.70114/acmsr.2025.3.1.P177

	110	6.85	4.84	3.95	3.06	2.28
8	10	53.25	37.66	30.75	23.82	17.75
	20	26.63	18.83	15.37	11.91	8.88
	40	14.79	10.46	8.54	6.62	4.93
	110	4.84	3.42	2.80	2.17	1.61
12	10	43.48	30.75	25.10	19.45	14.49
	20	21.74	15.37	12.55	9.72	7.25
	40	12.08	8.54	6.97	5.40	4.03
	110	3.95	2.80	2.28	1.77	1.32

5. Summary

This article simulates and analyzes the coverage performance of the ground geometry relationship of the GNSS-R payload carried by low orbit satellites. Through the joint-simulation method of STK and Matlab, analyze and summarize the visibility of specular reflection signals and sea surface coverage performance under different scenarios such as orbital heights, antenna beam numbers, working hours, measure spatial resolutions, single satellite or multi-satellite networking etc. The results show that the low orbit GNSS-R payload can efficiently detect global marine environmental elements. A 4-beam antenna can achieve global sea coverage greater than 80% and measurement accuracy better than 10cm under single satellite, which has practical value. At the same time, the data results can be used to evaluate the coverage efficiency and measurement accuracy for different payload designs. Furthermore, by using multi satellite networking or compatible navigation receivers to receive signals from different GNSS constellations, can improve coverage efficiency and measurement accuracy.

References

[1] YANG Dongkai, LI Xiaohui, WANG Feng. Analysis of Application Status of GNSS Reflected Signal in Ocean Remote Sensing. Radio Engineering, 2019, 49(10): 843 − 848.

[2] WANG Wei. Analysis on the Application of Global Navigation Satellite Reflected Signals in Ocean Remote Sensing. Journal of Ocean Technology, 2017, 36(1): 6.

[3] Unwin M, Gleason S, Brennan M. The Space GPS Reflectometry Experiment On the UK Disaster Monitoring Constellation Satellite BIOGRAPHY. 16th International Technical Meeting of the Satellite Division of the Institute of Navigation, 2003.

[4] Foti G, Gommenginger C, Jales P, et al. Spaceborne GNSS Reflectometry for Ocean Winds: First Re-sults from the UK TechDemoSat-1 Mission. Geophysical Research Letters, 2015, 42(13): 5435-5441.

[5] Ruf C S, Atlas R, Chang P S, et al. New ocean winds satellite mission to probe hurricanes and tropical convection. Bulletin of the American Meteorological Society, 2016, 97(3): 385–395.

[6] YANG Dongkai, WANG Feng, LI Weiqiang, et al. Simulation analysis of Beidou reflection events based on LEO satellites. Chinese Journal of Radio Science, 2015, 30(3): 409–416.

[7] LIU Congliang, BAI Weihua, XIA Junming, et al. Simulation study of spaceborne GNSS-R event. Geomatics and Information Science of Wuhan University, 2018, 43(6): 826–831, 839.

[8] BAI Weihua, ZHAO Danyang, XIA Junming, et al. Statistical Analysis of Simulated Space-Borne GNSS-R Data in Different Antenna Coverage and Installation Condition. Geomatics and Information Science of Wuhan University, 2023, 48(3): 386-395.

[9] ZHANG Pengfei, CHANG Jianlong, HU Chunsheng. Simulation analysis of GNSS space coverage performance. Telecommunication Engineering, 2018, 58(6): 675 − 681.

[10] WANG Feng, YANG Dongkai, ZHANG Bo. Spatiotemporal Performance of Spaceborne Global Navigation Satellites System Reflectometry. Journal of Electronics & Information Technology, 2022, 44(2): 760-766.